Rusty old stars: a source of the missing interstellar iron?

Journal Item

The Astrophysical Journal Letters, 717:L92–L97, 2010 July 10 doi:10.1088/2041-8205/717/2/L92

RUSTY OLD STARS: A SOURCE OF THE MISSING INTERSTELLAR IRON?

I. McDonald[1], G. C. Sloan[2], A. A. Zijlstra[1], N. Matsunaga[3], M. Matsuura[4,5], K. E. Kraemer[6], J. Bernard-Salas[2], and A. J. Markwick[1]

[1] Jodrell Bank Centre for Astrophysics, Alan Turing Building, Manchester, M13 9PL, UK; iain.mcdonald-2@jb.man.ac.uk, albert.zijlstra@manchester.ac.uk, andrew.markwick@manchester.ac.uk
[2] Cornell University, Astronomy Department, Ithaca, NY 14853-6801, USA; sloan@isc.astro.cornell.edu
[3] Institute of Astronomy, University of Tokyo, 2-21-1 Osawa, Mitaka, Tokyo 181-0015, Japan; matsunaga@ioa.s.u-tokyo.ac.jp
[4] UCL-Institute of Origins, Astrophysics Group, Department of Physics and Astronomy, University College London, Gower Street, London WC1E 6BT, UK
[5] UCL-Institute of Origins, Mullard Space Science Laboratory, University College London, Holmbury St. Mary, Dorking, Surrey RH5 6NT, UK; mikako@star.ucl.ac.uk
[6] Air Force Research Laboratory, Space Vehicles Directorate, Hanscom AFB, MA 01731, USA
Received 2010 April 9; accepted 2010 May 19; published 2010 June 18

ABSTRACT

Iron, the universe's most abundant refractory element, is highly depleted in both circumstellar and interstellar environments, meaning it exists in solid form. The nature of this solid is unknown. In this Letter, we provide evidence that metallic iron grains are present around oxygen-rich asymptotic giant branch stars, where it is observationally manifest as a featureless mid-infrared excess. This identification is made using *Spitzer Space Telescope* observations of evolved globular cluster stars, where iron dust production appears ubiquitous and in some cases can be modeled as the only observed dust product. In this context, FeO is examined as the likely carrier for the 20 μm feature observed in some of these stars. Metallic iron appears to be an important part of the dust condensation sequence at low metallicity, and subsequently plays an influential role in the interstellar medium. We explore the stellar metallicities and luminosities at which iron formation is observed, and how the presence of iron affects the outflow and its chemistry. The conditions under which iron can provide sufficient opacity to drive a wind remain unclear.

Key words: circumstellar matter – globular clusters: individual (NGC 362, NGC 5139, NGC 5927) – infrared: stars – stars: AGB and post-AGB – stars: mass-loss – stars: winds, outflows

1. INTRODUCTION

Iron is the sixth most abundant element in the universe, and the most abundant refractory element. It is observed to be highly depleted in both interstellar and circumstellar environments (Savage & Bohlin 1979; Maas et al. 2005; Delgado Inglada et al. 2009), and must therefore predominantly exist in an unknown solid form. Iron may be incorporated in other dust grains, primarily silicates, though these are usually iron-poor (Gail & Sedlmayr 1999; Kemper et al. 2002). Alternatively, iron may form a metallic condensate (Kemper et al. 2002; Verhoelst et al. 2009).

Dust grains form around evolved stars by condensation from the gas phase, either directly, or onto molecular "seeds". Individual dust species can usually be identified by distinct infrared emission bands. In oxygen-rich environments, amorphous or crystalline forms of silicates, spinels, and corundum are observed to form, while carbon-rich environments give rise to amorphous carbon (amC), graphite, and SiC. Metallic iron grains, however, produce featureless infrared emission which can be difficult to differentiate from other sources, particularly amorphous carbon dust. Iron has hitherto only been inferred as a likely component of oxygen-rich dusty winds (Kemper et al. 2002; Verhoelst et al. 2009), but never positively identified.

Previous observational studies (McDonald et al. 2009; Boyer et al. 2009) of giant stars in globular clusters have found a featureless contribution in addition to the flux emanating from the star's photosphere, which has been attributed to an unidentified circumstellar dust species. We herein show that this dust species is metallic iron.

2. EVIDENCE FOR DUST EMISSION

2.1. Observations

Our sample consists of 35 highly evolved, (strongly) pulsating stars in globular clusters (Sloan et al. 2010, Paper I), observed using the *Spitzer Space Telescope* Infrared Spectrograph (IRS). These long-period variable stars lie near or above the red giant branch tips of 19 Galactic globular clusters, which range in metallicity from [Fe/H] = –1.62 to –0.10. Observed with *Spitzer's* low-resolution modules, the spectra cover $\lambda = 5.2$–$38\ \mu$m with a resolving power of $R \sim 60$–120.

One carbon-rich star (Lyngå 7 V1) is discounted, leaving a sample of 34 stars. Of these, silicate features at 10 and 20 μm are seen in 24 objects, implying oxygen-rich chemistry. More pertinently, the remaining 10 stars either have very weak silicate features or appear to be "naked".

JHKL-band light curves are also available (Paper I) for 25 of our 34 objects, which allows us to construct the photometric fluxes of these objects at the pulsation phase of their IRS spectrum.

Figure 1 shows the $L-[8]$ color for these objects, where the 8 μm photometry was derived by convolving the IRS spectrum with the *Spitzer* IRAC 8 μm filter. A truly naked photosphere should have $L - [8] \approx 0$, once interstellar reddening has been taken into account[7] (cf. Boyer et al. 2008). All 25 stars, however, have a positive color. This implies a flux excess at 8 μm which cannot be caused by commonly assumed dust species (silicates,

[7] We here assume $E(L-[8]) = 0.017E(B-V)$, after Whittet (1992) and Flaherty et al. (2007).

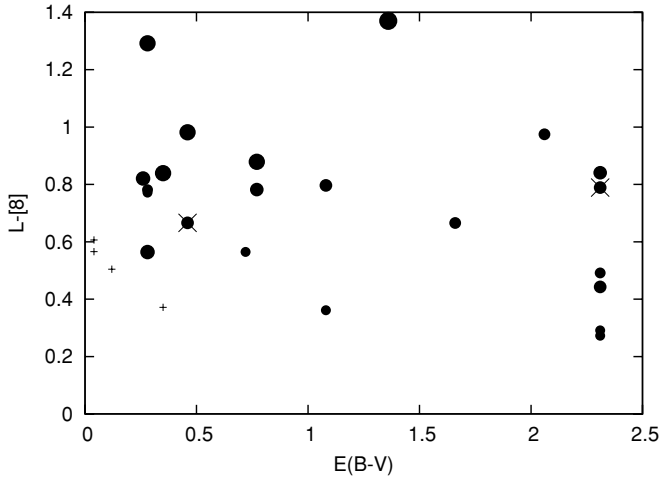

Figure 1. Extinction-corrected $L - [8]$ colors in our sources. Plus signs show stars with pure iron dust, filled circles show stars also hosting silicate dust (symbol size is proportional to strength of emission). Crosses show stars exhibiting a strong 20 μm feature. Color does not vary significantly with $E(B - V)$, showing that this is not merely a reddening effect.

alumina) under normal conditions of temperature and grain size. This excess flux at long wavelengths is confirmed by comparison to MARCS photospheric model spectra (Gustafsson et al. 1975, 2008; McDonald et al. 2009) as shown below.

From our sample, four example stars have been selected for detailed modeling: NGC 5927 V3, a highly evolved asymptotic giant branch (AGB) star with a strong, narrow, 10 μm silicate feature; NGC 6352 V5, a less luminous giant star with unusual dust features; and NGC 362 V2 and NGC 5139 V42, "naked" RGB-tip or AGB stars showing optical TiO bands (indicating they are oxygen-rich) and infrared dust excesses, but no silicate features (Smith et al. 1999; McDonald et al. 2009; Boyer et al. 2009).

2.2. Fitting the Observations

For a dust-free comparison, we use a stellar atmosphere model created using the MARCS code (Gustafsson et al. 1975, 2008) at 3500 K, [Fe/H] = –1.0, [α/Fe] = +0.3 (see McDonald et al. 2009 for details of these models). Being very similar objects near the giant branch tip, we expect the effective surface temperature below the dust-producing zone to be 3750 $\pm$ ~250 K. We use the near-infrared flux to fit the photospheric continuum. A low-temperature, metal-rich model therefore represents an intentional bias toward a model with a more-luminous infrared spectrum compared to its near-infrared flux. This reduces the calculated excess to rule out disparity between the modeled and real photospheric spectra.

Figure 2 shows the observed spectra, alongside fits to the stellar wind contribution using DUSTY (Nenkova et al. 1999). Using the MARCS model atmosphere as an input, we fit a stellar wind model using metallic iron grains (Ordal et al. 1988). For each model, we assume a radiatively driven wind; and a standard Mathis–Rumpl–Nordsieck grain size distribution (Mathis et al. 1977), given by $n(a) = a^{-q}$, $q = 3.5$ for $a = 5$–250 nm.

We correct for interstellar reddening using the absorption profiles from McClure (2009). We further assume that $A_V = 3.2E(B - V)$ and that $A_V/A_K = 7.75$. $E(B - V)$ values for NGC 362, 5927, and 6352 are from Harris (1996), $E(B - V) = 0.10$ is assumed for ω Cen, based on Harris (1996) and McDonald et al. (2009). The correction applied is thus quite small and negligibly different from that applied in Paper I.

NGC 362 V2 and ω Cen V42 are best fit with a dust shell truncated to an outer radius (r_{outer}) of ~100 times the inner radius (r_{inner} = the dust formation radius). (Normally, fits are extended to $r_{outer}/r_{inner} \gtrsim 1000$.) This suppresses the flux at $\lambda > 30\,\mu$m. A similar effect can also be achieved by using a grain distribution with fewer large grains: both effects may be in play (we only model a truncated shell here). The strength, and indeed existence of, this suppression depends crucially on the subtraction of the infrared background (caused by Galactic interstellar medium and other cluster objects). While every effort has been made to make sure this has been done correctly, we cannot be conclusively sure that such a suppression and thus truncation exist.

In NGC 5927 V3 and NGC 6352 V5, we also observe other dust species, which emit at $\lambda > 8\,\mu$m. Identified species include silicates (magnesium-rich olivines and pyroxenes) at 10 and 20 μm and amorphous alumina (Al_2O_3) at 11–15 μm (optical constants from Draine & Lee 1984; Begemann et al. 1997). Related crystalline minerals with a smaller degree of amorphization are likely responsible for the sharp 9.6 and 13.1 μm features seen in NGC 6352 V5 (Sloan et al. 2003). Note that the fit to NGC 5927 V3 produces a fairly good match to the 10 μm feature, but at a wavelength which is too red. This can be caused by a number of factors, including grain size and porosity (Voshchinnikov & Henning 2008). The 20 μm feature has an unknown carrier: a promising candidate is magnesio-wüstite ($Mg_xFe_{1-x}O$; see, e.g., Posch et al. 2002; Lebzelter et al. 2006; Paper I). This provides a good fit to the feature in NGC 6352 V5. The comparatively red peak wavelength seen in NGC 6352 V5 further suggests that $x \approx 0$; i.e., that it is near-pure FeO (Henning et al. 1995). We return to this feature later.

We could not fit a single-temperature dust model to these two stars, implying that the dust species are not in thermal contact with each other. Iron and alumina were fit at temperatures of ~1000 K. In NGC 6352 V5, silicates and FeO were fit at ~450 K; in NGC 5927 V3, the strong 10 μm peak suggests mainly glassy silicates, which we fit at ~400 K.

Table 1 lists our fitted parameters, including dust temperatures at the outer and inner edges of the dust envelope (T_{outer}, T_{inner}) and the size of the envelope used (r_{outer}/r_{inner}, $r_{inner} \sim 2\,R_*$). We do not include mass-loss rates, as explained at the end of this section.

2.3. Alternative Sources of Excess

Featureless infrared excess can be produced by a variety of circumstellar material. This can take the form of free–free emission, emission from shells of molecular gas (a "molsphere"; e.g., Tsuji 2000), extremely large silicate grains, or amorphous carbon grains. Figure 3 shows modeled fits for these possible emission sources, modeled in an identical way to the iron fits listed above.

Ionization in a chromosphere or shock fronts propagating through the outer atmosphere can give rise to free–free emission, as observed by radio observations toward Galactic Miras (Reid & Menten 1997). The optical depth of free–free emission in a region of thickness r can be calculated as

$$\tau_\nu = \int_r 3.28 \times 10^{-7} \left(\frac{T_e}{10^4 \mathrm{K}}\right)^{-1.35} \nu_{\mathrm{GHz}}^{-2.1} \left(\frac{n_e}{\mathrm{cm}^{-3}}\right)^2 \frac{\delta r}{\mathrm{pc}}, \quad (1)$$

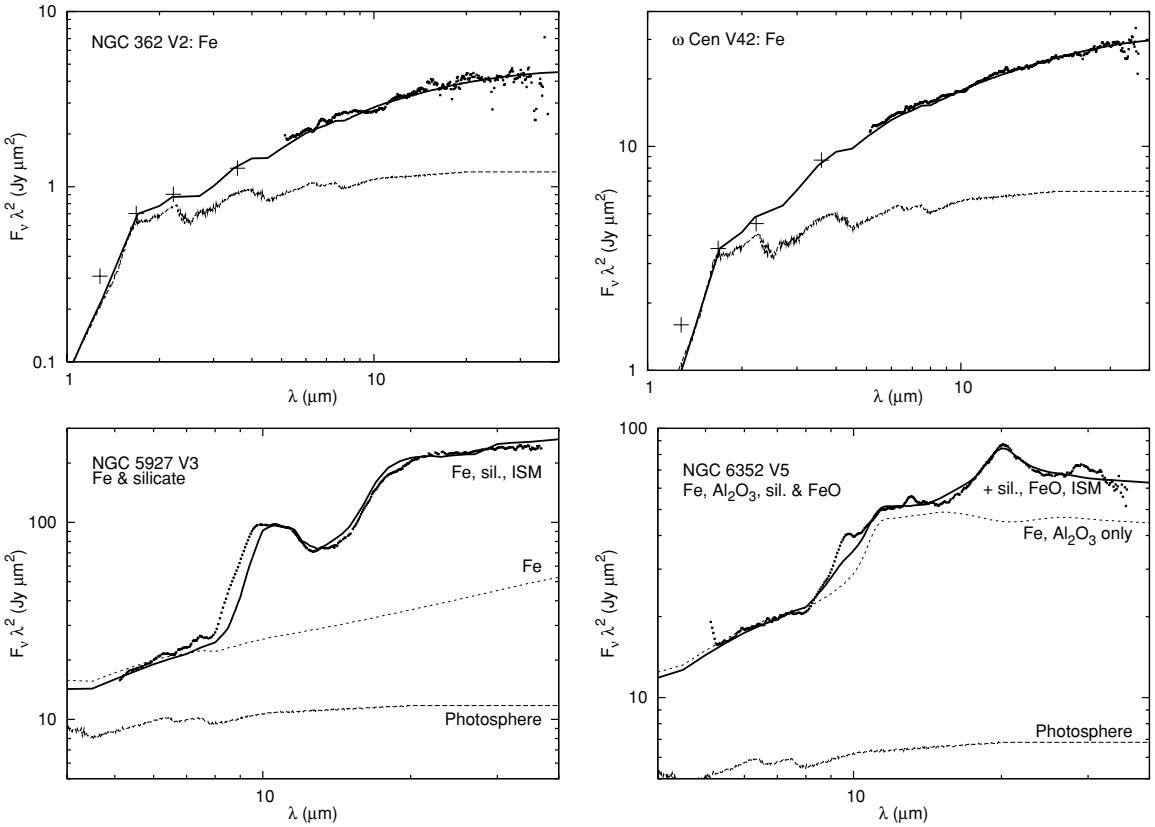

Figure 2. Modeled dust contributions (solid lines) to *Spitzer* IRS spectra (black dots) and *JHKL* photometry (black pluses), which has been corrected to the pulsation phases of the IRS spectra. The dashed line is a MARCS model denoting the photospheric contribution. The bottom two panels include the extra indicated contributions from Al_2O_3, silicates, and FeO (dotted lines).

Table 1
Parameters of DUSTY Models Presented in Figure 2.

Parameter	NGC 362 V2	ω Cen V42	NGC 5927 V3		NGC 6352 V5	
Assumed luminosity ($L_\odot$)	1826	1862	2000		2000	
Assumed [Fe/H]	−1.16	−1.62	−0.37		−0.70	
Assumed $E(B-V)$	0.05	0.10	0.45		0.21	
References	1, 3	2	4		4	
Wind component			A	B	A	B
Composition	100% Iron	100% Iron	100% Iron	100% Silicate	96% Fe 4% Al_2O_3	70% Silicate 30% FeO
$T_{\text{inner dust envelope edge}}$ (K)	800	1000	1100	400	1000	450
$T_{\text{outer dust envelope edge}}$ (K)	194	173	...	...	...	...
$r_{\text{outer}}/r_{\text{inner}}$	50	120	1000	1000	100	100
Optical depth at 0.55 μm	0.28	0.70	0.55	0.45	1.05	0.12

References. (1) Boyer et al. 2009; (2) McDonald et al. 2009; (3) $E(B-V)$ from Harris 1996; (4) luminosity estimated, metallicity from Harris 1996.

where the electron density, n_e, is recoverable from the electron temperature, T_e, via the Saha equation. At low frequencies, where $\tau_\nu \gg 1$, the emission scales as $F_\nu \propto \nu^{-2}$ for an isothermal, isobaric region; and $F_\nu \propto \nu^{-0.6}$ for an isothermal wind expanding with constant velocity. For ω Cen V42, we find our spectrum would require $\tau_\nu = 1$ at 3–4 μm, and that $F_\nu \propto \nu^{-1.6}$ for $\tau_\nu \gg 1$. This more-closely approximates an isobaric density profile, which would be difficult to achieve in an expanding wind. Very similar conditions would have to exist in all 34 of our stars, as the shape of their spectra are very similar.

An isobaric chromosphere producing a spectrum with this optical depth cannot exist except in the following case: the wind must be mostly ionized ($\gtrsim$6000 K) *and* either the chromosphere extends to an unphysical radius ($\gtrsim 70\,R_\odot$) and/or the mass-loss rate becomes unphysical ($\gtrsim 10^{-5.5}\,M_\odot$ yr^{-1}) for a thermally expanding wind. Departing from an isobaric state makes conditions even more prohibitive. While chromospheres may be present in these stars, this infrared excess is not seen in chromospherically active stars that are less evolved (McDonald & van Loon 2007; Boyer et al. 2009). In V42, circumstellar ionization appears dominated by pulsation shocks. Reid & Menten (1997) show that, for Galactic Miras, the temperature and density increases provided by shocks in the outer atmosphere are insufficient to produce an ionized layer that would be

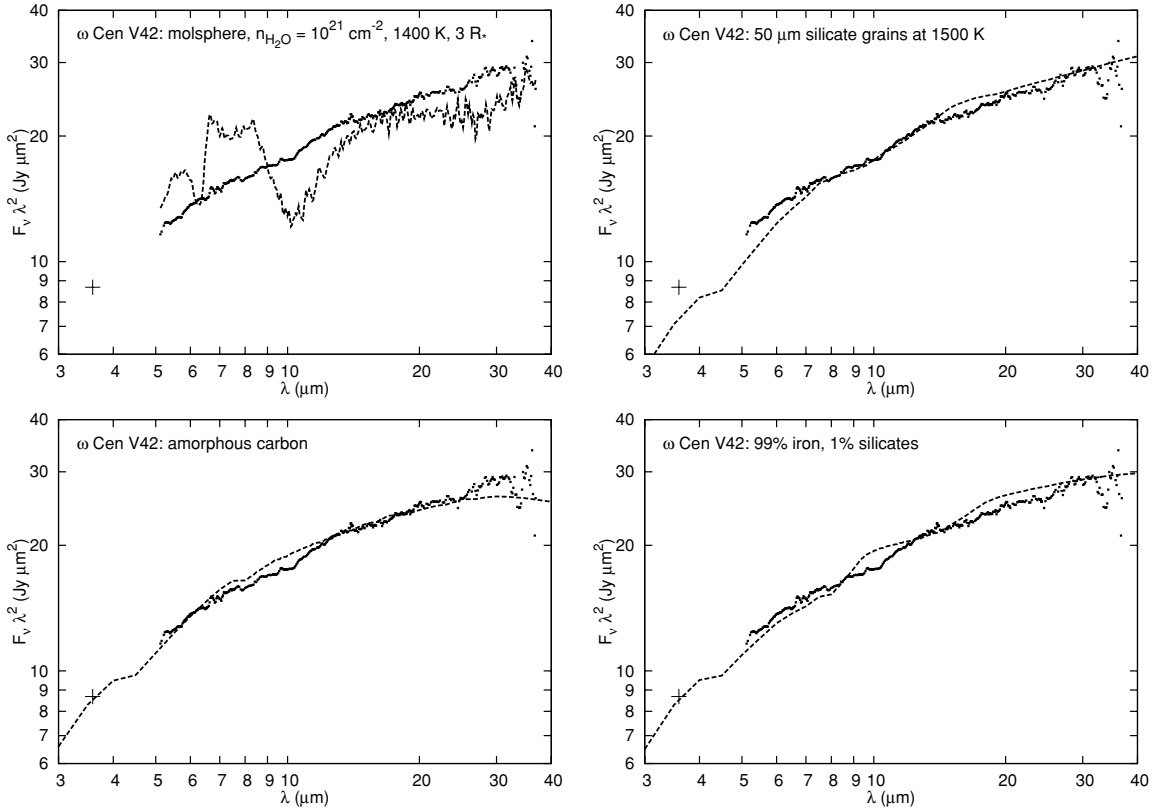

Figure 3. Fits to the *Spitzer* IRS spectrum of ω Cen V42 using alternative emission sources. In each panel, the following is shown—dots: IRS spectrum; plus sign: phase-corrected *L*-band photometry; dotted line: fit for indicated grain composition or emission mechanism.

optically thick in the infrared. We thus rule out free–free emission as a dominant contributor to our spectra.

The molsphere creates a dense "forest" of molecular lines. Water lines are the most important, and cause emission throughout the spectrum, but mainly in the 6–8 μm and $> 20\,\mu$m regions. This emission is seen in some of our example stars (Paper I). However, the water bands in our spectra are very weak compared to stars with naked molspheres (e.g., β Peg—Tsuji et al. 1997). Gas-phase model emission spectra (Figure 3), created from the line list of Partridge & Schwenke (1997) using SpectraFactory[8] (Cami et al. 2010), fail to reproduce the flatness of the spectrum for any reasonable combination of temperature and column density. Figure 3 shows the highest column density we consider feasible, and even this contains $\sim 10^{-7}\,M_\odot$ of water or $\sim$0.01% of the star's oxygen. Furthermore, most molsphere host stars still require an extra opacity source (such as iron grains) providing flux at 6–8 μm (Verhoelst et al. 2009). Infrared molecular emission should therefore not make a significant contribution to our spectra.

Of the commonly considered dust species only metallic iron and amC produce a featureless infrared continuum that matches the observed "naked" spectra. Other dust species (e.g., graphite) produce either strong spectral features or inflections which do not fit observed spectra. Spectral features can be damped by unusual conditions, notably exceptionally large grains (Höfner 2008): these cannot simultaneously reproduce both the excess at $\lambda < 8\,\mu$m and $\lambda > 20\,\mu$m at the observed levels (Figure 3) and are not expected in metal-poor stars where grain growth may be hampered by a lack of constituent elements.

Observationally, amC can also provide an acceptable fit to our example stars over most of the spectrum. The remaining discrepancies may be fixable by fine-tuning the wind parameters (grain size, density distributions, temperatures, background subtraction, etc.). Detection of amC as dominant dust species in an oxygen-rich environment would be unexpected. In giant stars, carbon and oxygen are bound into CO near the stellar surface, locking away the least abundant element. The remaining majority element, either carbon or oxygen, dominates the dust chemistry. CO may be dissociated in atmospheric shock waves or by chromospheric UV irradiation (Beck et al. 1992). This can lead to the production of small amounts of other carbon-rich molecules: mainly CO_2 (observed in our stars: see Paper I), but also HCN and CS (Duari et al. 1999). Small quantities of carbon-rich dust may then form (Höfner & Andersen 2007), though oxygen-rich dust production is still expected to be dominant. In our sample, however, the featureless component often appears to be the dominant species, and no evidence for oxygen-rich dust is found.

Having ruled out the alternatives, we conclude that the source of the dust excess must be iron grains, and that these must dominate the condensed material in some stars. If we naïvely assume identical populations of spherical grains, the fraction of warm silicates in the "naked" stars being $\lesssim$1% of the iron content (Figure 3; the same would be true at a $\lesssim$3% level for an amC component). The silicate fraction may increase if iron grains are made smaller and oblate, thus presenting a higher cross section per unit mass: extreme needle-like grains are required if silicates are to become the dominant dust species by mass. As we do not know the grain shape, it becomes difficult to estimate a mass-loss rate for an iron wind. Spherical grains produce unfeasibly

[8] http://spectrafactory.net

low expansion velocities of order $\sim$m s^{-1} for a pure iron wind; expansion velocities for NGC 5927 V3 and NGC 6352 V5 were not calculated as the model assumes a zero initial velocity for both temperature components, which will not be the case if they form at different radii. The mass-loss rates and expansion velocities can also be significantly modified by altering, e.g., the grain size or density (single crystal versus conglomerate), but reasonable changes still fail to produce feasible values, except for extremely elongated grains.

This implies that iron alone may not be able to drive a dusty wind in these stars. Other factors may also accelerate the wind. These could include small amounts of amorphous carbon (Höfner & Andersen 2007); energy deposition either from shocks created by stellar pulsations (Bowen 1988), or magnetic reconnection (Pijpers & Hearn 1989); increased opacity from circumstellar molecular gas (Elitzur et al. 1989); stellar pulsation, either by direct acceleration or dissipation of shocks; or line-driving of H I or Ca II atoms, or H_2O molecules (e.g., Elitzur et al. 1989; Bowen 1989). The driving mechanism is thus likely to be complex, with radiation pressure on metallic iron being only one of several accelerants which drive matter from the star. Obtaining an accurate radial profile of the wind's outflow velocity will be crucial in determining which factors dominate this acceleration.

3. DISCUSSION

3.1. The Fate of Iron and Iron-oxide Grains

Efficient production of metallic iron by oxygen-rich AGB stars would explain several iron depletions. Gas-phase depletion of iron extends to the interstellar medium (Savage & Bohlin 1979). Iron grains contribute to infrared emission from this medium (Chlewicki & Laureijs 1988) and iron is seen to be destroyed in shocks (Lebouteiller et al. 2008). Iron is also depleted by >90% in the gas phase of planetary nebulae (Delgado Inglada et al. 2009). Direct evidence for iron condensation in AGB winds comes from depletion patterns in binary post-AGB stars. In these stars, the wind is captured in a circumbinary disk, from where gas re-accretes onto the star. These stars show large depletions of refractory elements, with iron being among the most depleted (Maas et al. 2005) thus indicate a history of iron-rich dust production.

The 20 μm feature, seen in NGC 6352 V5, is also observed in NGC 5927 V1 and Terzan 5 V6. It has a width (FWHM) of $\sim$3μm and a line-to-continuum ratio up to 50%. This feature has previously been seen in low mass-loss stars; it correlates with the presence of an 11 μm shoulder, and 13.1 and 28 μm peaks (Little-Marenin & Little 1988; Sloan et al. 2003). The related peaks are also present in our sample, and we confirm that the 20 μm feature disappears for more evolved (i.e., more luminous) stars. The 20 μm and associated features are barely detectable in the naked stars, strongest in stars with weak silicate emission and disappear when silicates dominate (Figure 4). This suggests they are produced either during the formation or destruction of silicate grains. The identification of the feature with $Mg_xFe_{1-x}O$ is unconfirmed mainly because it does not predict the associated features, but the proposed identifications for those (corundum, pyroxenes; Sloan et al. 2003) do not provide good fits at 20 μm, making it plausible that a range of minerals form under these conditions. We suggest that these features may be caused by the chemical modification of silicate grains: silicate grains which adsorb iron into the lattice have higher opacity, and can be heated until the iron-bearing component dissociates from the grain (Woitke 2006). This is expected to occur at any radius from the star at which dust formation is efficient (Gail & Sedlmayr 1999). In this model, metallic iron is produced first, but at higher metallicity and mass-loss rates, the iron becomes partly incorporated into other grain types including iron-oxide and iron-containing silicates.

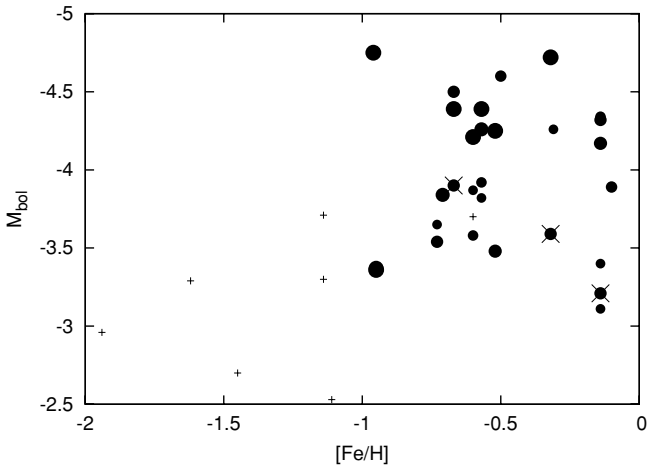

Figure 4. Variation of dust properties with bolometric magnitude and metallicity. Symbols as shown in Figure 1.

Studies of inclusions within meteoric primitive solar system material have traced dust grains to specific origins in AGB stars, supernovae and novae, through their isotopic ratios (Zinner 2003; Messenger et al. 2005). Recently, the first pre-solar iron-oxide grain has been identified (Floss et al. 2008). The iron and oxygen isotopic ratios in it are indicative of an origin in an AGB star. This supports the hypothesis that AGB stars are a source of interstellar iron dust, and have contributed to the solar system's iron content.

3.2. The Dust Condensation Sequence at low [Fe/H]

Figure 4 shows the variation of dust types (see Paper I) with bolometric magnitude and metallicity. Silicate-rich winds are only seen at high luminosity or high metallicity, with iron dominating the outflow in lower-luminosity, lower-metallicity stars. This indicates that the dust condensation sequence depends on metallicity and luminosity. Gail & Sedlmayr (1999) show that, under equilibrium conditions, iron is only expected to condense before silicates in regions with high gas pressure. If this applies to our stars, it implies high gas pressure at low metallicity and/or low luminosity, as may be expected if the outflow velocities where iron condenses (at the outside edge of the molsphere) are very low. Under non-equilibrium conditions, grain growth chemistry is strongly controlled by kinetics (Tachibana et al. 2009), which may favor the formation of iron.

In Gail & Sedlmayr (1999), silicates form before iron at lower densities and temperatures. The restriction of silicates toward higher metallicity and luminosity (Figure 4) suggests that their circumstellar envelopes are more extended, favoring silicates. Silicate production is expected to increase with both stellar metallicity and luminosity (van Loon 2000).

4. CONCLUSIONS

Using mid-infrared spectra and photometry, we have shown that there is a considerable amount of unattributed infrared flux in a large selection of globular cluster giants. Through

radiative transfer modeling, we deduce that this flux is most likely due to metallic iron grains forming in a truncated stellar wind, corroborated by a potential identification of FeO with the 20 μm emission feature. The production of metallic iron seems to become more dominant at lower metallicity, suggesting that the dust condensation sequence is fundamentally different in metal-poor objects. Large-scale production of iron grains and iron oxide in AGB stars can explain iron depletion in the gas and solid phases of the post-AGB stars and planetary nebulae; as well as isotopic ratios in FeO grains in meteorites. While iron increases opacity in oxygen-rich winds, it remains unclear whether it can dominate the driving of metal-poor winds. Future observations to determine outflow velocities in these stars should help determine the driver of these stellar winds.

This Letter uses observations made using the *Spitzer Space Telescope*, operated by JPL, California Institute of Technology under NASA contract 1407 and supported by NASA through JPL (contract number 1257184). We thank Martha Boyer for her helpful comments.

REFERENCES

Beck, H. K. B., Gail, H., Henkel, R., & Sedlmayr, E. 1992, A&A, 265, 626
Begemann, B., Dorschner, J., Henning, T., Mutschke, H., Guertler, J., Koempe, C., & Nass, R. 1997, ApJ, 476, 199
Bowen, G. H. 1988, in Pulsation and Mass Loss in Stars, ed. R. Stalio & L. A. Willson (Astrophys. Space Sci. Lib. 148; Dordrecht: Kluwer), 3
Bowen, G. H. 1989, in IAU Colloq. 106, Evolution of Peculiar Red Giant Stars, ed. H. R. Johnson & B. Zuckerman (Cambridge: Cambridge Univ. Press), 269
Boyer, M. L., McDonald, I., van Loon, J. T., Woodward, C. E., Gehrz, R. D., Evans, A., & Dupree, A. K. 2008, AJ, 135, 1395
Boyer, M. L., et al. 2009, ApJ, 705, 746
Cami, J., van Malderen, R., & Markwick, A. J. 2010, ApJS, 187, 409
Chlewicki, G., & Laureijs, R. J. 1988, A&A, 207, L11
Delgado Inglada, G., Rodríguez, M., Mampaso, A., & Viironen, K. 2009, ApJ, 694, 1335
Draine, B. T., & Lee, H. M. 1984, ApJ, 285, 89
Duari, D., Cherchneff, I., & Willacy, K. 1999, A&A, 341, L47
Elitzur, M., Brown, J. A., & Johnson, H. R. 1989, ApJ, 341, L95
Flaherty, K. M., Pipher, J. L., Megeath, S. T., Winston, E. M., Gutermuth, R. A., Muzerolle, J., Allen, L. E., & Fazio, G. G. 2007, ApJ, 663, 1069
Floss, C., Stadermann, F. J., & Bose, M. 2008, ApJ, 672, 1266
Gail, H., & Sedlmayr, E. 1999, A&A, 347, 594
Gustafsson, B., Bell, R. A., Eriksson, K., & Nordlund, A. 1975, A&A, 42, 407
Gustafsson, B., Edvardsson, B., Eriksson, K., Jørgensen, U. G., Nordlund, Å., & Plez, B. 2008, A&A, 486, 951
Harris, W. E. 1996, ApJ, 112, 1487
Henning, T., Begemann, B., Mutschke, H., & Dorschner, J. 1995, A&AS, 112, 143
Höfner, S. 2008, A&A, 491, L1
Höfner, S., & Andersen, A. C. 2007, A&A, 465, L39
Kemper, F., de Koter, A., Waters, L. B. F. M., Bouwman, J., & Tielens, A. G. G. M. 2002, A&A, 384, 585
Lebouteiller, V., Bernard-Salas, J., Brandl, B., Whelan, D. G., Wu, Y., Charmandaris, V., Devost, D., & Houck, J. R. 2008, ApJ, 680, 398
Lebzelter, T., Posch, T., Hinkle, K., Wood, P. R., & Bouwman, J. 2006, ApJ, 653, L145
Little-Marenin, I. R., & Little, S. J. 1988, ApJ, 333, 305
Maas, T., Van Winckel, H., & Lloyd Evans, T. 2005, A&A, 429, 297
Mathis, J. S., Rumpl, W., & Nordsieck, K. H. 1977, ApJ, 217, 425
McClure, M. 2009, ApJ, 693, L81
McDonald, I., & van Loon, J. T. 2007, A&A, 476, 1261
McDonald, I., van Loon, J. T., Decin, L., Boyer, M. L., Dupree, A. K., Evans, A., Gehrz, R. D., & Woodward, C. E. 2009, MNRAS, 394, 831
Messenger, S., Keller, L. P., & Lauretta, D. S. 2005, Science, 309, 737
Nenkova, M., Ivezić, Ž., & Elitzur, M. 1999, in LPI Contrib. 969, Thermal Emission Spectroscopy and Analysis of Dust, Disks, and Regoliths, ed. A. Sprague, D. K. Lynch, & M. Sitko (Houston, TX: Lunar and Planetary Institute), 20
Ordal, M. A., Bell, R. J., Alexander, R. W., Jr., Newquist, L. A., & Querry, M. R. 1988, Appl. Opt., 27, 1203
Partridge, H., & Schwenke, D. W. 1997, J. Chem. Phys, 106, 4618
Pijpers, F. P., & Hearn, A. G. 1989, A&A, 209, 198
Posch, T., Kerschbaum, F., Mutschke, H., Dorschner, J., & Jäger, C. 2002, A&A, 393, L7
Reid, M. J., & Menten, K. M. 1997, ApJ, 476, 327
Savage, B. D., & Bohlin, R. C. 1979, ApJ, 229, 136
Sloan, G. C., Kraemer, K. E., Goebel, J. H., & Price, S. D. 2003, ApJ, 594, 483
Sloan, G. C., et al. 2010, ApJ, submitted (Paper I)
Smith, V. V., Shetrone, M. D., & Keane, M. J. 1999, ApJ, 516, L73
Tachibana, S., Nagahara, H., Ozawa, K., Tamada, S., & Ogawa, R. 2009, in Lunar and Planetary Inst. Tech. Rep. 40, Lunar and Planetary Institute Science Conference Abstracts, 2512
Tsuji, T. 2000, ApJ, 540, L99
Tsuji, T., Ohnaka, K., Aoki, W., & Yamamura, I. 1997, A&A, 320, L1
van Loon, J. T. 2000, A&A, 354, 125
Verhoelst, T., van der Zypen, N., Hony, S., Decin, L., Cami, J., & Eriksson, K. 2009, A&A, 498, 127
Voshchinnikov, N. V., & Henning, T. 2008, A&A, 483, L9
Whittet, D. C. B. 1992, Dust in the Galactic Environment (Bristol: Institute of Physics Publishing)
Woitke, P. 2006, A&A, 460, L9
Zinner, E. K. 2003, in Treatise on Geochemistry, Vol. 1, ed. A. M. Davis (Amsterdam: Elsevier), 17